Nonisothermal Crystallization Behavior of Melt-Intercalated Polyethylene-Clay Nanocomposites

Q. Yuan,[1,2] S. Awate,[1,2] R. D. K. Misra[1,2]

[1]*Center for Structural and Functional Materials, University of Louisiana at Lafayette, Lafayette, Louisiana 70504-4130*
[2]*Department of Chemical Engineering, University of Louisiana at Lafayette, Lafayette, Louisiana 70504-4130*

Received 17 January 2006; accepted 10 May 2006
DOI 10.1002/app.24852
Published online in Wiley InterScience (www.interscience.wiley.com).

ABSTRACT: The influence of nanoclay particles on the nonisothermal crystallization behavior of intercalated polyethylene (PE) prepared by melt-compounding was investigated. It is observed that the crystallization peak temperature (T_p) of PE/clay nanocomposites is slightly but consistently higher than the neat PE at various cooling rates. The half-time ($t_{0.5}$) for crystallization decreased with increase in clay content, implying the nucleating role of nanoclay particles. The nonisothermal crystallization data are analyzed using the approach of Avrami (Polymer 1971, 12, 150), Ozawa (Polym Eng Sci 1997, 37, 443), and Mo and coworkers (J Res Natl Bur Stand 1956, 57, 217), and the validity of the different kinetic models to the nonisothermal crystallization process of PE/clay nanocomposites is discussed. The approach developed by Mo and coworkers successfully explains the nonisothermal crystallization behavior of PE and PE/clay nanocomposites. The activation energy for nonisothermal crystallization of neat PE and PE/clay nanocomposites is determined using the Kissinger (J Res Natl Bur Stand 1956, 57, 217) method. © 2006 Wiley Periodicals, Inc. J Appl Polym Sci 102: 3809–3818, 2006

Key words: polyethylene; nanocomposites; differential scanning calorimeter; crystallization

INTRODUCTION

Polyolefins, a class of materials of large industrial interest, are one of the fastest growing classes of thermoplastics due to their good balance of favorable processability, mechanical properties, and chemical resistance. Some polyolefins, such as polyethylene (PE), has been extensively used in both packaging and engineering applications. However, their inadequate stiffness and brittleness restrict their versatile applications to some extent. Compounding with micro- or nanosize inorganic particles is a simple, effective, and economical method to improve the mechanical and thermal properties of polymeric materials. The structure–property relationship of microsize inorganic particle-filled polymer blends have been comprehensively studied.[1–6]

Comparing to the neat polymer, polymer nanocomposites generally exhibit improved properties, such as mechanical properties, reduced thermal expansion coefficient, and higher thermal stability.[7–11] Our recent work has indicated that the addition of clay significantly improves the scratch resistance of polypropylene (PP).[12] Thus, during the last decade, polymer nanocomposites have received significant attention both in the industry and in the academia. Among the different nanoparticles used in polymer nanocomposites, clay has been widely studied because two types of polymer/clay nanocomposites are possible, namely intercalated and exfoliated, allowing the tailoring of the properties.

The study of crystallization in a crystalline polymer micro- or nanocomposite is of particular significance, because crystallization may have a strong influence on the structure of composites and thereby the mechanical properties, such as tensile and impact strength. For example, it was noted that the extent of intercalation increased with the crystallization temperature, and the size of spherulite decreased on increasing the clay content in maleic anhydride grafted PP/clay nanocomposites.[13] The crystallization behavior of semicrystalline polymers and conventional filler-reinforced polymer composites has been studied in some detail.[14–26] The factors identified to influence the crystallization behavior of polymers include size,[14] shape,[19] and content of filler.[14]

Generally, isothermal and nonisothermal kinetics analyses are used to study the crystallization behavior of crystalline polymers. Comparing with isothermal crystallization, the study of nonisothermal crystallization is much more complicated, since one more variable, i.e., the temperature as function of time must be considered. Also, the study of nonisothermal

Correspondence to: R. D. K. Misra (dmisra@louisiana.edu).

crystallization in polymer composites is of greater practical significance because processing techniques always involve nonisothermal conditions. Recently, the nonisothermal crystallization kinetics of various polymers was investigated theoretically and experimentally.[27–33] Some models were proposed to quantitatively describe the crystallization kinetics.[29–31] In general, the surface of filler particles acts as a nucleation site for semicrystalline polymer, thereby altering the amount or type of crystals. For example, under identical conditions, PP-carbonate composites have more β-crystal PP than in PP-talc composites, because the carbonate particles exhibit stronger β-crystal nucleation effect than the talc particles.[34] More recently, Perrin-Sarazin et al.[35] observed that the crystallization kinetics (crystallization temperature and rates) and structure of PP is not only related to the clay-content but also to the PP-clay interactions. In the absence of coupling agent, the crystallization of PP occurred at higher temperature and at a rate greater than neat PP, but the crystallization behavior was nearly similar to neat PP in the presence of coupling agent. Xu et al.[16] observed the nucleation effect of montmorillonite (MMT) on the crystallization of PE in PE/MMT nanocomposites synthesized by *in situ* polymerization. However, suppression and nucleation effects coexisted in the intercalated material leading to longer induction time and higher overall crystallization rate.

Recently, nonisothermal crystallization kinetics of polymer nanocomposites has been studied in some detail in systems including poly(ethylene oxide) (PEO)/MMT,[20] PP/carbon nanotubes,[26] polyamide 66/clay,[36] PP/surface-treated SiO_2,[15] isotactic PP/$CaCO_3$,[19] *in situ* polymerization PE/clay,[16] poly(trimethylene terephthalate)/clay,[37] PP/MMT,[18] and polyamide 6/clay.[38,39] Generally speaking, there are two mutually opposite effects of nanoclay particles on the crystallization behavior: nucleating ability and growth retardation, which are related to the content and dispersion state of clay. PEO/MMT [20] and polyamide 6/clay[39] have both been observed to exhibit similar trend in regard to the influence of clay on the crystallization behavior of polymer nanocomposites, at lower clay concentrations, i.e., the crystallization kinetics was enhanced; while at higher clay concentrations, the rate of crystal growth was decreased.

Generally, the preparation methods of polymer/clay nanocomposites include *in situ* polymerization, solvent intercalation, and melt-compounding. Furthermore, the processing conditions strongly affect the crystallization behavior of polymer/clay nanocomposites. The nonisothermal crystallization behavior of PE/clay prepared by *in situ* polymerization has been investigated by Xu et al.,[16] but the behavior of the melt-compounded PE/clay nanocomposites remains unclear. Thus, the objective of the present work is to examine the nonisothermal crystallization kinetics of neat and PE/4 and 8 wt % clay nanocomposites processed by melt blending using differential scanning calorimetry (DSC). The kinetics is subsequently analyzed using the theoretical approach of Avrami, Ozawa, and Mo and coworkers[40–42] for nonisothermal crystallization. Finally, the activation energy describing the nonisothermal crystallization process is calculated based on Kissinger method.[43]

EXPERIMENTAL

Materials and physical properties

The polymer used in this study is commercially available grade of high density polyethylene (PE) copolymer produced by Solvay (formal product name: ethane-hexene-1 copolymer). It is developed for blow molding automotive fuel tanks and other large parts, where the finished part demands environmental stress crack resistance. This grade has a melt flow rate of 9 g/10 min at 190/2.16 kg. A natural montmorillonite (MMT) clay surface modified with dimethyl dialkyl ammonium (Nanomer I.44P, Nanocor) was used as the reinforcement filler. The nanocomposites were prepared by mixing the appropriate amounts in twin screw extruder followed by injection molding of bars.

Microscopy

The dispersibility and intercalation of PE into the clay layers was studied by transmission electron microscopy (TEM). Sections of 100–200 nm were cut using a Leica ultra-microtome equipped with a diamond knife and collected in a trough filled with water and placed directly on 400-mesh copper grids. Transmission electron micrographs were taken with Hitachi H-7600 at an acceleration voltage of 100 kV.

Wide-angle X-ray diffraction

The wide-angle X-ray diffraction (WAXD) patterns were analyzed on a Scintag, XDS 2000 X-ray diffractometer, operating at 43 kV and 21 mA using Cu Kα radiation of wavelength 1.54 Å as the X-ray source. Samples were scanned at a rate of 1.0°/min in the 2θ range of 3°–40°.

Differential scanning calorimetry

The crystallization behavior of polymer nanocomposites was studied with differential scanning calorimetry (DSC, TA Instruments). Samples of 10 ± 0.01 mg were used. Nonisothermal crystallization tests were performed at cooling rate of 2.5, 5, 10, and 20 K/min, respectively. The samples were initially melted at

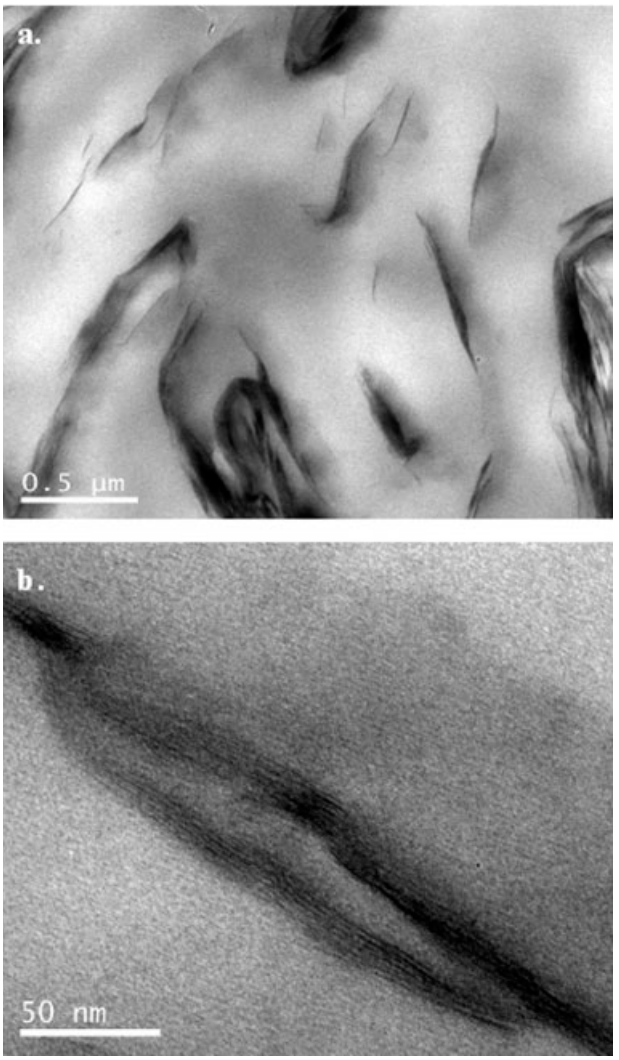

Figure 1 Transmission electron micrographs showing (a) uniform dispersion of clay nanoplatelets; and (b) high-magnification micrograph showing well-intercalated clay layers at 4 wt % loading.

453 K for 5 min to erase all previous thermal history. All measurements were carried out in nitrogen-containing atmosphere.

RESULTS AND DISCUSSION

TEM of PE-4 wt % clay nanocomposite are presented in Figure 1. A uniform distribution [Fig. 1(a)] and intercalated structure [Fig. 1(b)] are observed in PE/clay nanocomposites.

The effects of clay on the crystallization behavior of PE were quantitatively analyzed through nonisothermal DSC experiments. Figure 2 shows the crystallization thermograms of PE and PE/clay nanocomposites at various cooling rates. From these plots, the crystallization temperature (T_c) and crystallization peak temperature (T_p) of neat PE and its nanocomposites can be determined. T_c and T_p are defined as the initial crystallization temperature and the peak maximum temperature, respectively. Also, the heat evolved during crystallization (ΔH_c) can be obtained; the results are summarized in Table I. It is noted that both T_c and T_p decrease marginally with

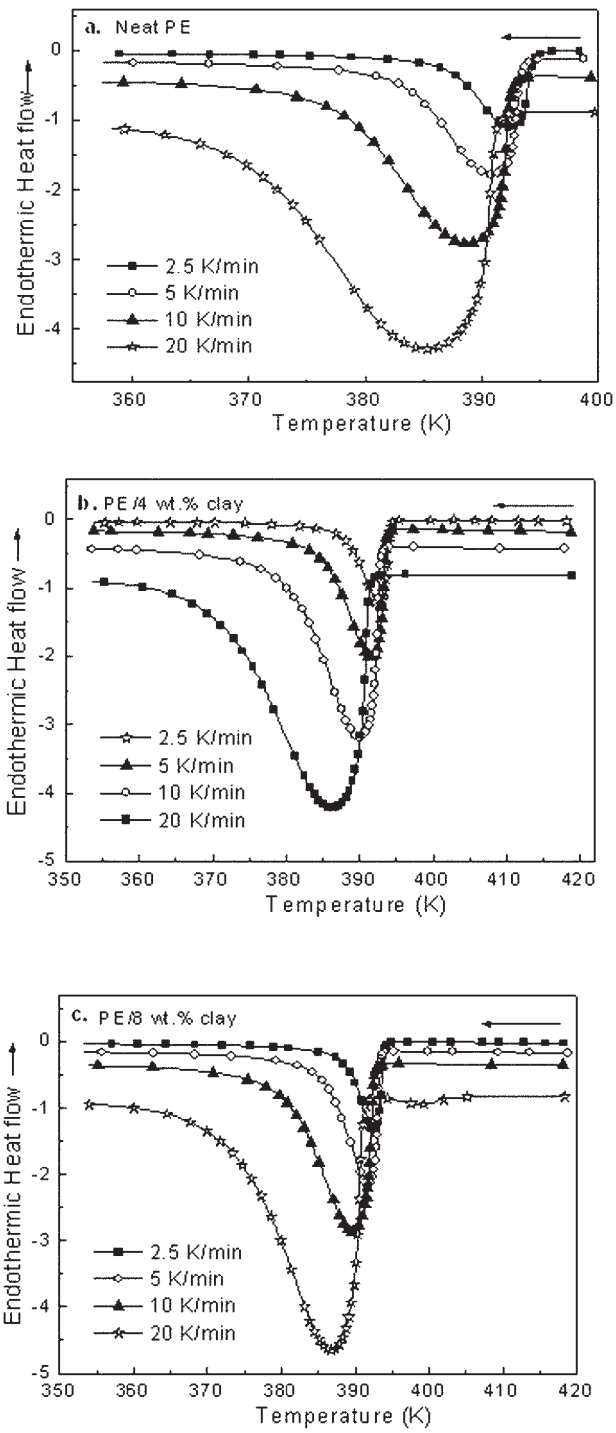

Figure 2 DSC thermograms of nonisothermal crystallization of PE-clay nanocomposites at various cooling rates of (a) neat PE, (b) PE-4 wt % clay, and (c) PE-8 wt % clay nanocomposites.

TABLE I
Values of the Heat Evolved During Crystallization (ΔH_c), the Crystallization Onset Temperature (T_c), the Crystallization Peak Temperature (T_p), and the Half Time of the Crystallization ($t_{0.5}$) for Neat PE and PE-Clay Nanocomposites at Various Cooling Rates

Material	Cooling rate (K/min)	ΔH_c[a] (J/g)	T_c (K)	T_p (K)	$t_{0.5}$ (min)
Neat PE	2.5	151.5	393.9	392.4	2.54
	5	157.9	393.0	390.8	1.58
	10	163.6	392.0	388.7	1.00
	20	185.9	390.7	385.1	0.74
PE-4% clay	2.5	135.1	393.8	392.6	2.47
	5	144.4	393.2	391.1	1.25
	10	140.4	392.5	389.4	0.97
	20	152.5	390.8	385.8	0.64
PE-8% clay	2.5	133.8	393.6	392.6	1.76
	5	136.5	393.1	391.1	1.38
	10	133.9	392.2	389.7	0.86
	20	142.8	390.6	386.1	0.62

[a] For 100 wt % polymer.

increasing cooling rate. For example, T_p of neat PE decreases about 7 K, when the cooling rate increases from 2.5 to 20 K/min. A similar behavior was observed for the PE/clay nanocomposites. This behavior is related to the fact that at lower cooling rate there is more time to overcome the nucleation energy barrier, consequently, the crystallization starts at higher temperature.[33] Figure 3 shows the relationship between crystallization peak temperature (T_p) and cooling rate for neat PE and PE/clay nanocomposites. It can be seen that the presence of clay in PE leads only to a slight increase in T_p. Comparing with our recent results on PP/clay nanocomposite,[44] the increase of crystallization peak temperature (T_p) of PP is significantly large for identical clay content and processing conditions. Fillon et al.[45] defined the nucleation efficiency, NE, of a given substance by eq. (1):

$$\mathrm{NE} = 100\frac{T_{\mathrm{CNA}} - T_{C1}}{T_{C2\,\max} - T_{C1}} \quad (1)$$

where T_{CNA} is the peak crystallization temperature of the polymer with the nucleating agent, T_{C1} is the crystallization temperature of the polymer to which no nucleating substances are added, and $T_{C2\max}$ is the optimum self-nucleation temperature ($T_{C2\max}$ of PE and PP is 406.95 and 437.65 K, respectively). On the basis of eq. (1), the nucleation efficiency of PE/4 wt % clay and PP/4 wt % clay nanocomposites at cooling rate of 10 K/min, is 3.3% and 21.7%, respectively. This implies that the role of clay as nucleating agent is much more pronounced in PP/clay nanocomposites, compared with that in PE/clay nanocomposites. Polarized light microscopy results indicated that the spherulite size of PP-crystals was significantly reduced, but the PE-crystals remain unaffected on incorporation of clay.[46,47] This difference in the nucleating ability between the two systems led to lowering of toughness in PE-clay system and increase in toughness in PP-clay system for identical clay content and processing conditions.

It is known that the nanoclay particles have both nucleation and suppression effects on the crystallization of polymer matrix. From X-ray diffraction studies, we believe that the reason for the lower change of crystallization temperature in PE as compared to PP is more likely related to the two mutually opposing effects: nucleating effect and suppression effect. The nucleating effect has a positive effect, while suppression effect has a negative effect, and is related to the clay content or *d*-spacing of clay layers. This is supported from the WAXD results. The clay used was same in both PE and PP systems. There are two peaks ($2\theta = 4.2$ and 6.7) belonging to nanoclay particles in PP/clay nanocomposites, while only one peak ($2\theta = 6.5$) is observed in the PE/clay nanocomposite for the identical clay content (Fig. 4). The

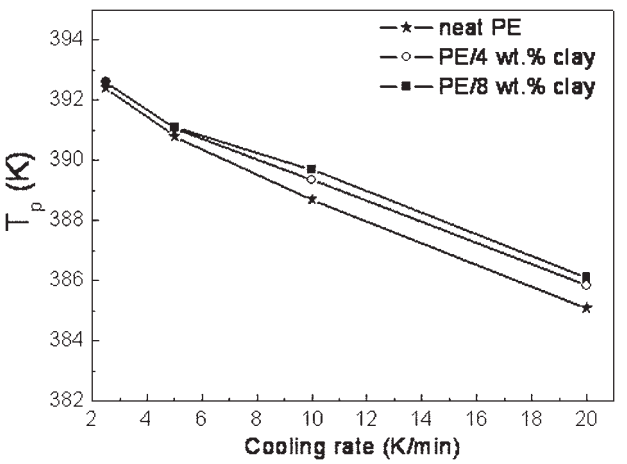

Figure 3 Crystallization peak temperature T_p versus cooling rate for PE-clay nanocomposites.

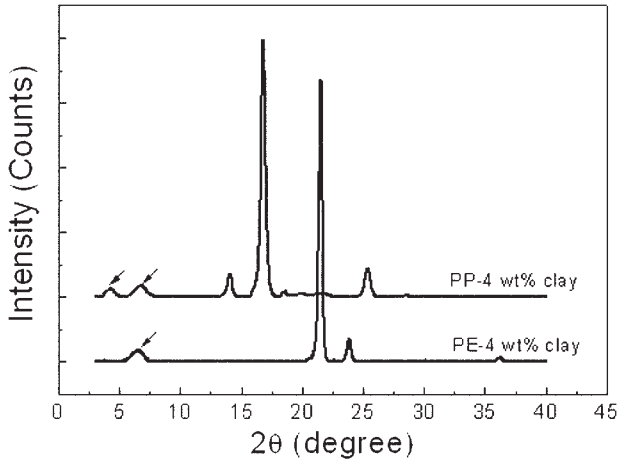

Figure 4 WAXD patterns of PE-4 wt % clay and PP-4 wt % clay nanocomposites. Arrows point to the (001) peaks of clay.

presence of lower angle peak in PP-clay nanocomposite suggests larger clay *d*-spacing formed in PP/clay nanocomposites, which helps in the mobility of PP chains during crystallization. As a consequence, the change of crystallization temperature in PP-clay nanocomposites is larger than PE-clay nanocomposites. This argument is further corroborated with the recent results of Xu et al.[16] They observed that exfoliated and intercalated polymer nanocomposites exhibited different crystallization behavior; the exfoliated PE/clay nanocomposite indicated higher crystallization temperature than the respective intercalated system.

The crystallinity (heat evolved during crystallization) of PE (Table I) decreased with the addition of nanoclay particles. The lower crystallinity may again be ascribed to the lower mobility of polymer chains in the PE matrix, which resulted from the presence of nanoclay particles. It is likely that the dispersed clay particles hinder the formation of large crystalline domains in the restricted and confined space. Interestingly, this behavior is similar to our observations in PP/glass bead blends.[48] In Figure 5, the relationship between the relative degree of crystallinity and the temperature for the PE/clay nanocomposites at various cooling rate is presented. The relative degree of crystallinity (X_t), as a function of crystallization temperature (T_c), was estimated from eq. (2):

$$X_t = \frac{\int_{T_0}^{T_t} (d\mathrm{H}_c/dT)dT}{\int_{T_0}^{T_\infty} (d\mathrm{H}_c/dT)dT} \quad (2)$$

where T_0 is the initial crystallization temperature and T_t and T_∞ are the crystallization temperature at time t and the ultimate crystallization temperatures, respectively. The dH_c is the enthalpy of crystallization released during an infinitesimal temperature range dT. According to different cooling rate (λ), the temperature parameters in Figure 5 can be converted into a time scale by using eq. (3):

$$t = (T_0 - T_t)/\lambda \quad (3)$$

where T_t is the temperature at crystallization time t, and λ is the cooling rate. The conversion from temperature to time is performed using a constant cooling rate.

Figure 6 shows the plots of the relative degree of crystallinity (X_t) as a function of time. It may be clearly seen that increasing the cooling rate reduces

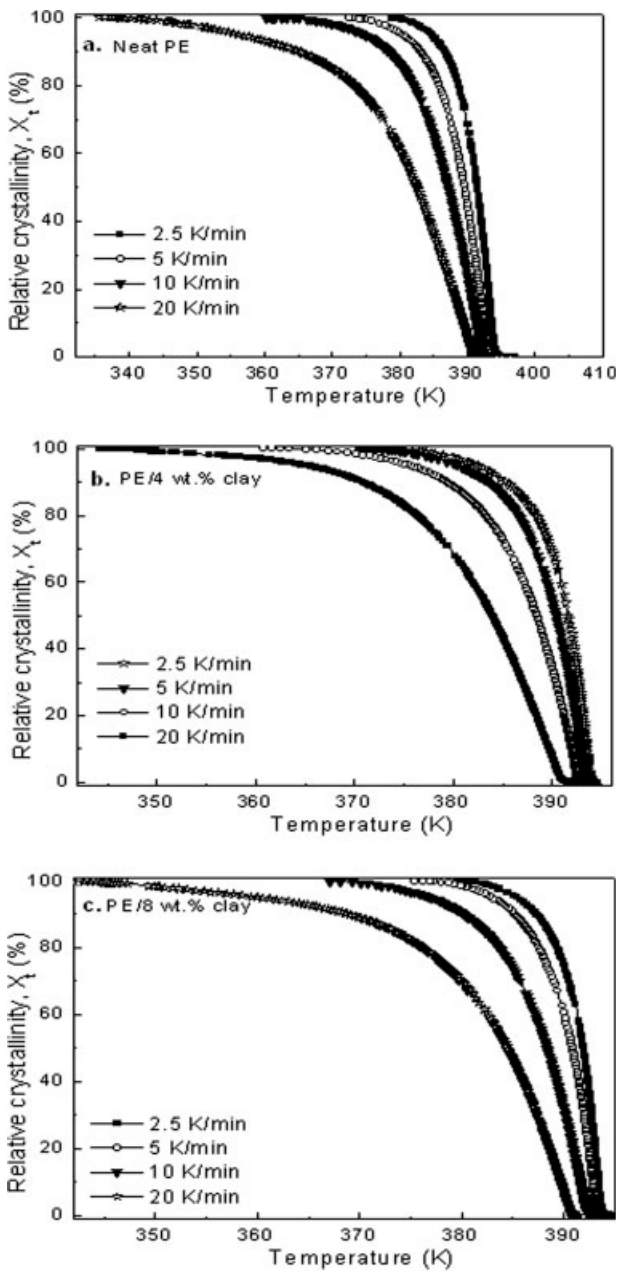

Figure 5 Variation of the relative crystallinity (X_t) with temperature for nonisothermal crystallization of (a) neat PE, (b) PE-4 wt % clay, and (c) PE-8 wt % clay nanocomposites.

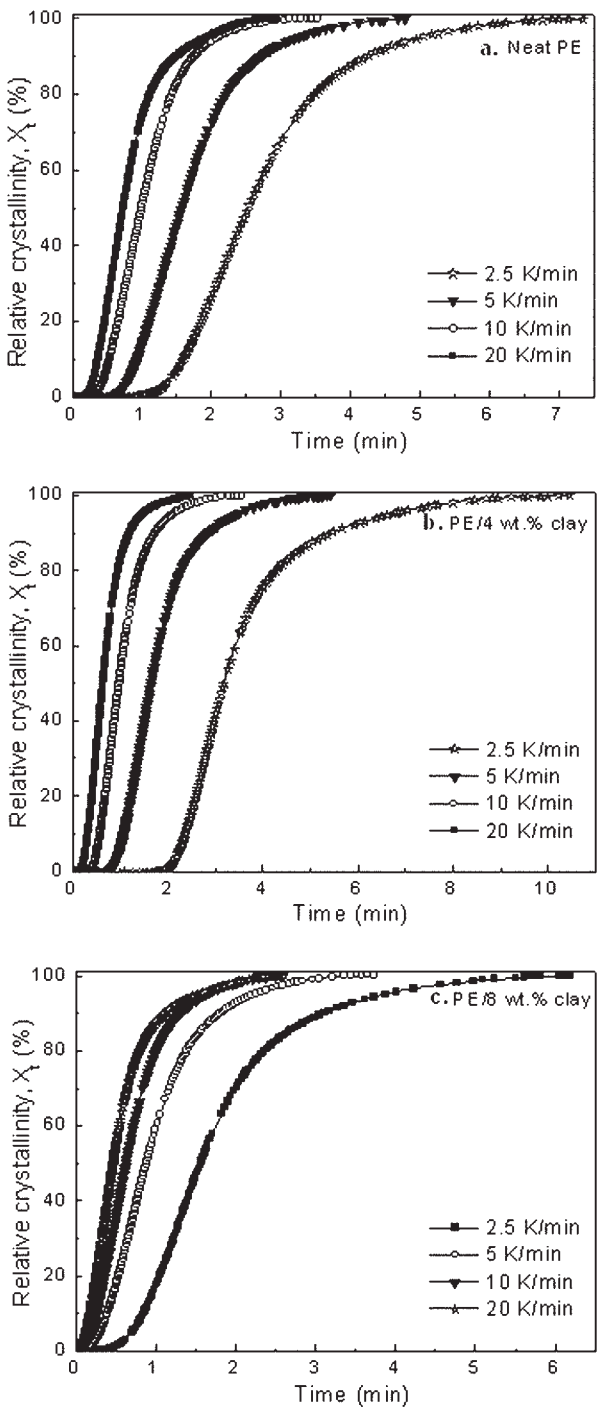

Figure 6 Variation of the relative crystallinity (X_t) with time for nonisothermal crystallization of (a) neat PE, (b) PE-4 wt % clay, and (c) PE-8 wt % clay nanocomposites.

the time required for the completion of crystallization. From these plots, an important parameter that can be derived is the half-time of crystallization ($t_{0.5}$), which is the value of the time from the onset of crystallization to the time at which X_t is 50%, and is listed in Table I. As expected, with increasing cooling rate, the crystallization half-time decreases, since $t_{0.5}$ is a measure of the crystallization rate. Furthermore, it is apparent from Table I that the value of half-time of crystallization for PE/clay nanocomposites at various cooling rates is lower than neat PE and decreases with increasing the content of clay. This can be explained as follows: nanoclay particles act as a heterogeneous nucleating agent to facilitate crystallization; and the higher the clay content, the greater is the nucleating effect. As a consequence, $t_{0.5}$ for crystallization tends to decrease with increasing clay content. In addition to the half-time of crystallization, other parameters, such as the kinetic rate coefficient, can also be used to characterize the nonisothermal crystallization kinetics of polymers. The common approach to analyze the isothermal crystallization kinetics is the Avrami equation [eq. (3)], which assumes that the relative crystallinity X_t developed with crystallization time t. The logarithmic form of eq. (4) is eq. (5).

$$X_t = 1 - \exp(-kt^n) \tag{4}$$

$$\ln[-\ln(1 - X_t)] = \ln k + n \ln(t) \tag{5}$$

where X_t, k, t, and n are the relative crystallinity, the rate constant, crystallization time, and Avrami exponent, respectively.[41]

Figure 7 shows the plots of $\ln[-\ln(1 - X_t)]$ vs. $\ln t$ for neat PE and PE/clay nanocomposites at various cooling rates. Each plot has a linear part corresponding to the early stage of crystallization and is followed by a gentle deviation at longer time. It is pertinent to mention that when eq. 4 is applied to nonisothermal crystallization, the parameters k, and n have different physical meaning because the temperature changes instantly in the nonisothermal crystallization. This affects the rates of both nucleation and growth process. Thus, in the present work, the Avrami analysis is inappropriate. Considering the nonisothermal character of the process, cooling rate (λ) is the factor that needs to be taken into consideration. On the basis of the mathematical derivation of Evans, Ozawa[41] modified the Avrami equation by incorporating the cooling rate (λ) and is given as:[42]

$$1 - X_t = \exp[-K(T)/\lambda^m] \tag{6}$$

where $K(T)$, m are the Ozawa crystallization rate constant, and exponent respectively. Equation (6) in the logarithmic form can be written as:

$$\ln[-\ln(1 - X_T)] = \ln K(T) - m \ln(\lambda) \tag{7}$$

Ozawa plots based on the nonisothermal crystallization data of PE and PE/clay nanocomposites for a series of temperatures are presented in Figure 8. In our study, the Ozawa plots of the nanocomposites

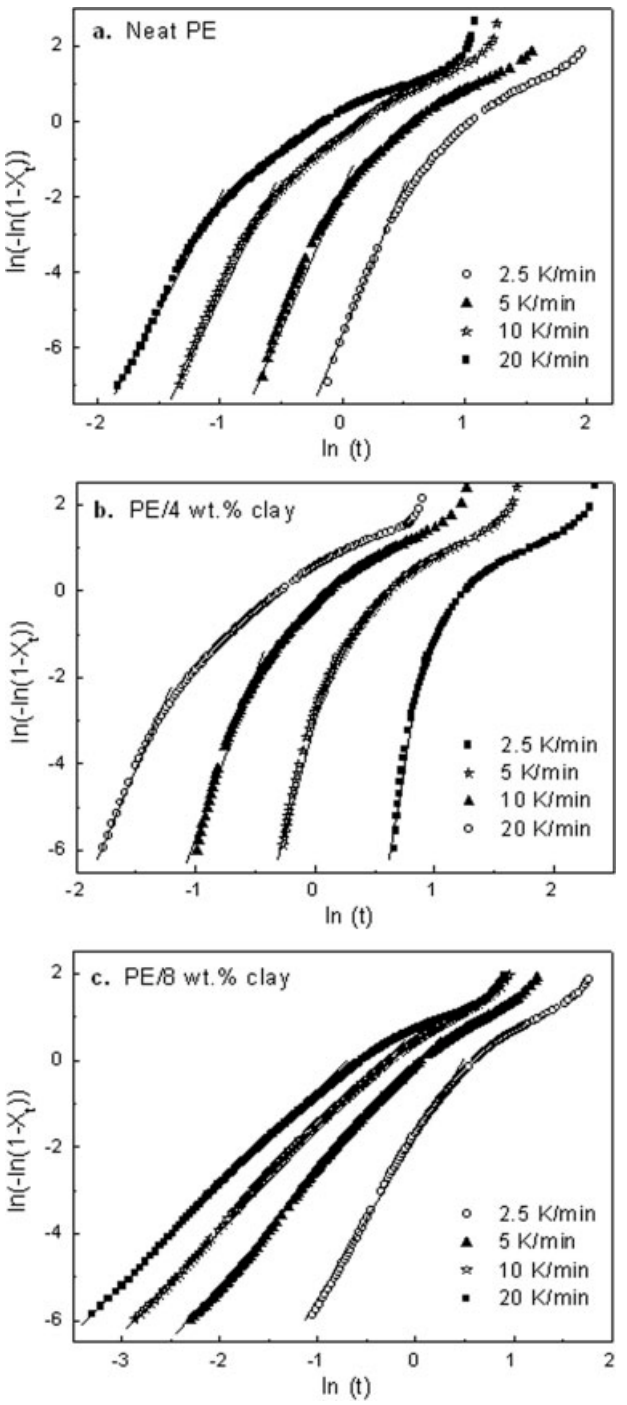

Figure 7 Plots of $\ln[-\ln(1 - X_t)]$ versus $\ln t$ for crystallization of (a) neat PE, (b) PE-4 wt % clay, and (c) PE-8 wt % clay nanocomposites at various cooling rates.

and neat PE show deviation from linearity when cooling rate varies from 2.5 to 20 K/min, implying that the Ozawa equation also fails to describe the nonisothermal crystallization of PE/clay nanocomposites, because the plots do not display a linear relationship. In this context, it is important to note that Ozawa equation ignores secondary crystallization. A modified method was proposed by Mo and coworkers[42] to describe the nonisothermal crystallization by combining the Avrami eq. (5) and Ozawa eq. (7). The modified equation is given as:

$$\ln \lambda = \ln F(T) - \alpha \ln t \tag{8}$$

where the kinetic parameter $F(T) = [K(T)/k]^{1/m}$ refers to the value of cooling rate selected at a unit crystal-

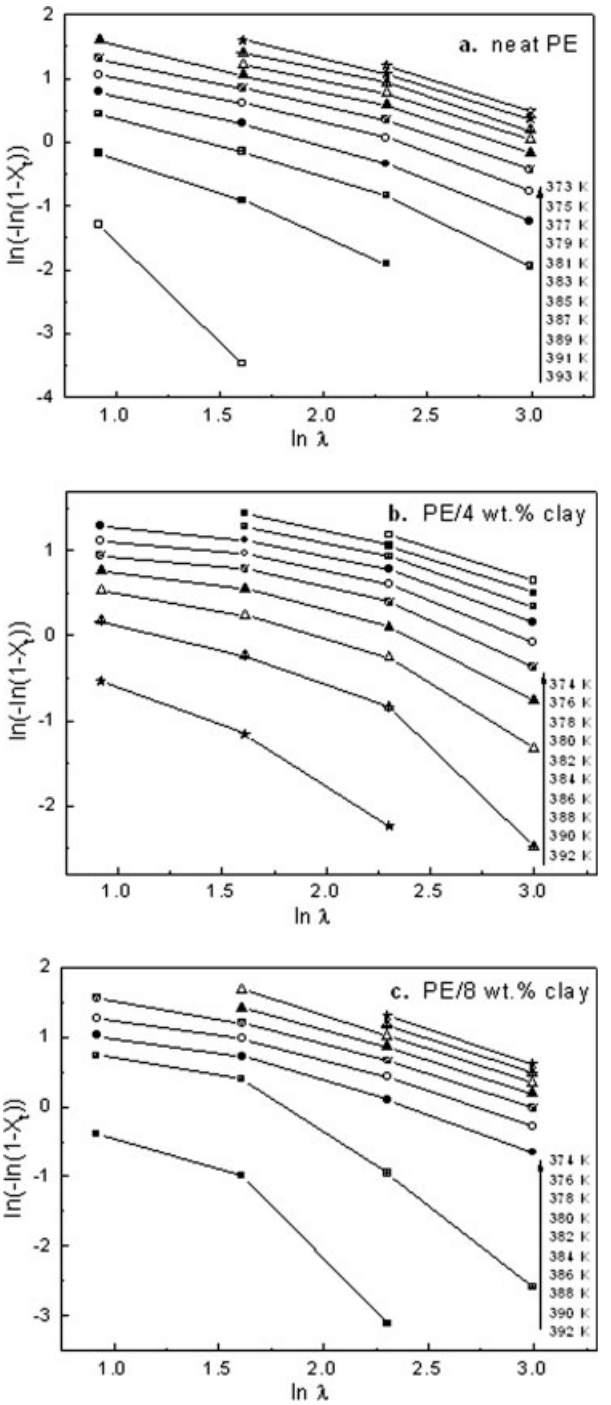

Figure 8 Ozawa plots of $\ln[-\ln(1 - X_t)]$ versus $\ln\lambda$ for crystallization of (a) neat PE, (b) PE-4 wt % clay, and (c) PE-8 wt % clay nanocomposites.

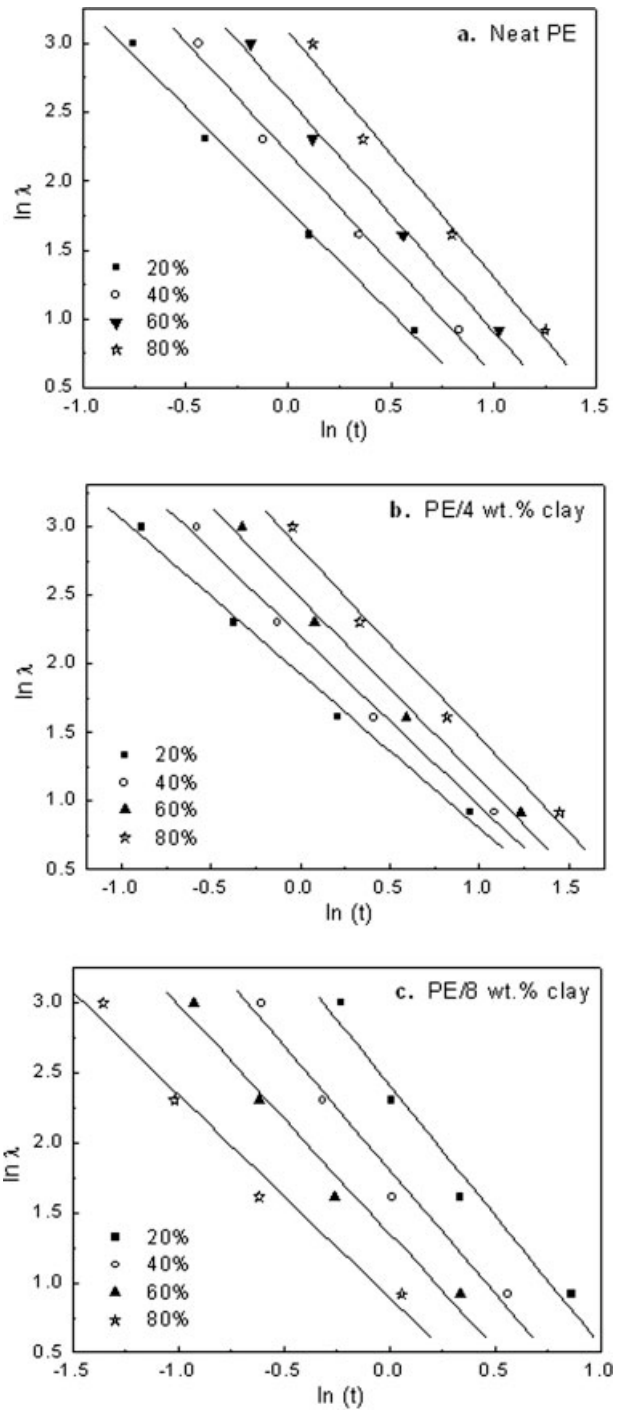

Figure 9 Plots of lnλ vs. ln*t* for (a) neat PE, (b) PE-4 wt % clay, and (c) PE-8 wt % clay nanocomposites.

lization time when the measured system has a certain degree of crystallinity, and $\alpha = n/m$ is the ratio of the Avrami exponent n to the Ozawa exponent m. Thus, at a given degree of crystallinity, from the plot of lnλ vs. ln*t* (Fig. 9), the values of α and $F(T)$ can be obtained by fitting linear slopes and determining intercepts of the lines, respectively. The results are listed in Table II. It can be seen from Table II that the value of α for neat PE varies from 1.49 to 1.78 and for PE/clay nanocomposite varies from 1.13 to 1.86. The deviation of the values of α for both neat PE and PE/clay nanocomposites is small, indicating that the eq. (8) proposed by Mo and coworkers satisfactorily describes the nonisothermal process of PE and PE/clay nanocomposites. Equation (8) was also used to describe the behavior of PP/clay nanocomposites,[44] PP/surface-treated SiO_2 nanocomposites,[15] nylon-11 nanocomposites,[49] and poly(trimethylene terephthalate)/clay nanocomposites.[37] The value of $F(T)$ systematically increases with the increase in the relative crystallinity for neat PE and PE/clay nanocomposites, and the $F(T)$ value of PE/clay nanocomposites are generally smaller than those of neat PE. Here, $F(T)$ mainly reflects the facilitation effect of nanoparticles clay on PE crystallization, the value of $F(T)$ decreases with the addition of nanoclay particles, indicating that the PE/caly nanocomposites can achieve the same degree of crystallinity faster than the neat PE. This implies faster kinetics of crystallization, and in agreement with our previous observation that the nanoclay particles act as a nucleating agent and accelerate the crystallization of PE (i.e., $t_{0.5}$ decreases with clay content; Table I).

Kissinger method[43] enables us to determine the activation energy (ΔE) for the transport of the macromolecular segments to the growing surface [eq. (9)]:

$$\frac{d[\ln(\lambda/T_p^2)]}{d(1/T_p)} = -\frac{\Delta E}{R} \tag{9}$$

where T_p, R, and λ are the peak temperature, the universal gas constant, and cooling rate, respectively. Figure 10 shows the plots based on the Kissinger method, and the slopes of the least-square lines drawn through these plots equal $\Delta E/R$, enabling determination of activation energy ΔE. The results of

TABLE II
Nonisothermal Crystallization Kinetic Parameters for Neat PE and PE-Clay Nanocomposites at Different Relative Degrees of Crystallinity by Combination of Avrami–Ozawa Equation and the Activation Energy (ΔE) Based on Kissinger Method

Material	X_t (%)	α	$F(T)$	Activation energy ΔE (kJ mol^{-1})
Neat PE	20	1.49	6.00	356.0
	40	1.61	9.07	
	60	1.69	13.44	
	80	1.78	21.83	
PE-4% clay	20	1.13	5.88	385.4
	40	1.24	9.05	
	60	1.32	11.91	
	80	1.37	17.04	
PE-8% clay	20	1.45	2.44	400.5
	40	1.64	3.87	
	60	1.76	6.09	
	80	1.86	11.14	

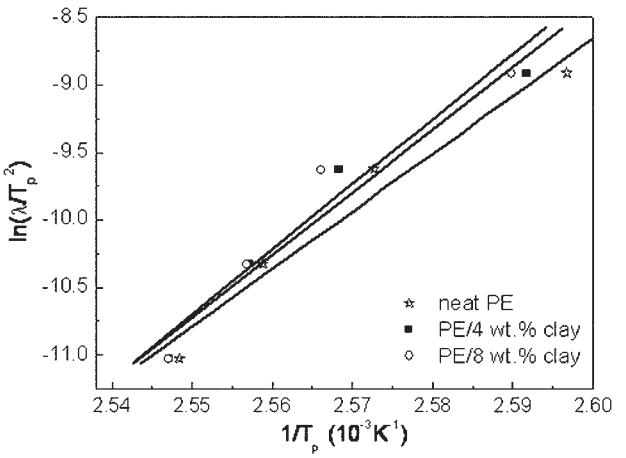

Figure 10 Determination of the activation energy (ΔE) describing the nonisothermal crystallization process for the PE and PE-clay nanocomposites based on Kissinger method.

ΔE are listed in Table II. The activation energies of nonisothermal melt crystallization of neat PE, PE/4 wt % clay, and PE/8 wt % clay nanocomposites are 356.0, 385.4, and 400.5 kJ/mol, respectively. In our recent results of PP/clay nanocomposites, the activation energy decreased with the addition of nanoclay particles. This can be discussed as follows. The crystallization process of polymers can be divided into two parts: (a) nucleation, which is related to the free energy barrier and (b) crystal growth whose rates is related to the activation energy for the transport of crystalline units across the phase. In the present study, the decrease of half-time indicates the lower free energy barrier for PE/clay nanocomposites compared to neat PE. However, for nanoclay particles, there are two mutually opposite effects on the crystallization behavior of the polymers: nucleating ability and growth retardation, which are related to the content and dispersion state of clay. The suppression effect of clay in PE/clay system is more pronounced than in PP/clay and this is consistent with the previous results, namely, the increase of crystallization peak temperature is less in PE/clay system. As a result, the value of ΔE in PE/clay system increases with the addition of nanoclay particles, while in PP/clay system it decreases slightly with the addition of nanoclay particles. This leads us to suggest that the experimentally determined activation energy is largely related to the growth process rather than to the initiation of the nucleation process.

CONCLUSIONS

1. Comparing with PP/clay nanocomposites, the crystallization temperature of PE increased less with the addition of clay, indicating the role of clay as nucleating agent was less pronounced in PE/clay nanocomposites, and this is also ascribed to the differences in *d*-spacing of clay layers in the two systems.
2. The nonisothermal crystallization behavior of neat PE and PE/clay nanocomposites were studied with DSC. The addition of clay to PE resulted in a decrease of the half-time for crystallization at various cooling rate, a behavior that is related to the nucleating effect of nanoclay particles.
3. Models, based on Avrami, Ozawa, and modified Avrami-Ozawa were used to examine the nonisothermal crystallization behavior. Both Avrami and Ozawa equations failed to provide an adequate description of the nonisothermal crystallization of PE and PE/clay nanocomposites. However, the method developed by Mo and coworkers successfully described the nonisothermal crystallization behavior of PE and PE/clay nanocomposites.
4. The activation energy for nonisothermal crystallization of PE and PE/clay nanocomposites determined from Kissinger method was found to increase with the presence of nanoclay particles.

References

1. Yuan, Q.; Jiang, W.; Zhang, H. X.; Yin, J. H.; An, L. J.; Li, R. K. Y. J Polym Sci Part B: Polym Phys 2001, 38, 1855.
2. Yuan, Q.; Jiang, W.; An, L. J.; Li, R. K. Y. Polym Adv Technol 2004, 15, 409.
3. Fu, Q.; Wang, G. H.; Shen, J. S. J Appl Polym Sci 1993, 49, 673.
4. Liang, J. Z.; Li, R. K. Y. Polymer 1999, 40, 3191.
5. Liang, J. Z.; Li, R. K. Y. Polym Compos 1998, 19, 698.
6. Zuiderduin, W. C. J.; Westzaan, C.; Huétink, J.; Gaymans, R. J. Polymer 2003, 44, 261.
7. Giannelis, E. P.; Krishnamoorti, R.; Manias, E. Adv Polym Sci 1999, 138, 107.
8. Nathani, H.; Dasari, A.; Misra, R. D. K. Acta Mater 2004, 52, 3217.
9. Hadal, R.; Yuan, Q.; Jog, J. P.; Misra, R. D. K. Mater Sci Eng A 2006, 418, 268.
10. Moussaif, N.; Groeninckx, G. Polymer 2003, 44, 7899.
11. Alexandre, M.; Dubois, P. Mater Sci Eng 2000, 28, 1.
12. Rao, R.; Mudaliar, A.; Yuan, Q.; Misra, R. D. K. Mater Sci Eng A 2006, 418, 292.
13. Maiti, P.; Nam, P. H.; Okamoto, M.; Kotaka, T.; Hasegawa, N.; Usuki, A. Polym Eng Sci 2002, 42, 1864.
14. Yuan, Q.; Jiang, W.; An, L. J.; Li, R. K. Y. J Polym Sci Part B: Polym Phys 2005, 43, 306.
15. Papageorgiou, G. Z.; Achilias, D. S.; Bikiaris, D. N.; Karayannidis, G. P. Thermochim Acta 2005, 427, 117.
16. Xu, J. T.; Wang, Q.; Fan, Z. Q. Eur Polym J 2005, 41, 3011.
17. Mitchell, C. A.; Krishnamoorti, R. Polymer 2005, 46, 8796.
18. Xu, W. B.; Ge, M. L.; He, P. S. J Polym Sci Part B: Polym Phys 2002, 40, 408.
19. Avella, M.; Cosco, S.; Di Lorenzo, M. L.; Di Pace, E.; Errico, M. E. J Therm Anal Calorim 2005, 80, 131.
20. Homminga, D. S.; Goderis, B.; Dolbnya, I.; Reynaers, H.; Groeninckx, G. Polymer 2005, 46, 11359.
21. Tjong, S. C.; Bao, S. P. J Polym Sci Part B: Polym Phys 2004, 42, 2878.

22. Wang, Y. M.; Shen, C. Y.; Li, H. M.; Li, Q.; Chen, J. B. J Appl Polym Sci 2004, 91, 308.
23. Hieber, C. A. Polymer 1995, 36 1455.
24. Tiganis, B. E.; Shanks, A.; Long, Y. J Appl Polym Sci 1996, 59, 663.
25. Velasco, J. L.; De Saja, J. A.; Martinez, A. B. J Appl Polym Sci 1996, 61, 125.
26. Leelapornpisit, W.; Ton-That, M. N.; Perrin-Sarazin, F.; Cole, K. C.; Denault, J.; Simard, B. J Polym Sci Part B: Polym Phys 2005, 43, 2445.
27. Supaphol, P.; Dangseeyun, N.; Srimoaon, P.; Nithitanakul, M. Thermochim Acta 2003, 406, 207.
28. Supaphol, P.; Dangseeyun, N.; Srimoaon, P. Polym Test 2004, 23, 175.
29. Yang, J.; McCoy, B. J. J Phys Chem B 2005, 109, 18550.
30. Yang, J.; McCoy, B. J.; Madras, G. J Chem Phys 2005, 122, 64901.
31. Yang, J.; McCoy, B. J.; Madras, G. J Chem Phys 2005, 122, 244905.
32. Philips, R.; Manson, J. A. E. J Polym Sci Part B: Polym Phys 1997, 35, 875.
33. Di Lorenzo, M. L.; Silvestre, C. Progr Polym Sci 1999, 24, 917.
34. McGenity, P. M.; Hooper, J. J.; Paynter, C. D.; Riley, A. M.; Nutbeem, C.; Elton, N. J.; Adams, J. M. Polymer 1992, 33, 5215.
35. Perrin-Sarazin, F.; Ton-That, M. T.; Bureau, M. N.; Denault, J. Polymer 2005, 46, 11624.
36. Kang, X.; He, S. Q.; Zhu, C. S.; Wang, L. Y.; Lü, L. Y. J Appl Polym Sci 2004, 95, 756.
37. Liu, Z. J.; Chen, K. Q.; Yan, D. Y. Eur Polym J 2003, 39, 2359.
38. Homminga, D. S.; Goderis, B.; Mathot, V. B. F.; Groeninckx, G. Polymer 2006, 47, 1630.
39. Fornes, T. D.; Paul, D. R. Polymer 2003, 44, 3945.
40. Avrami, M. J Chem Phys 1940, 8, 212.
41. Ozawa, T. Polymer 1971, 12, 150.
42. Liu, T. X.; Mo, Z. S.; Wang, S. E.; Zhang, H. F. Polym Eng Sci 1997, 37, 443.
43. Kissinger, H. E. J Res Natl Bur Stand 1956, 57, 217.
44. Yuan, Q.; Awate, S.; Misra, R. D. K. Eur Polym J, 2006, 42, 1994.
45. Fillon, B.; Lotz, B.; Thierry, A.; Wittmann, J. C. J Polym Sci Part B: Polym Phys 1993, 31, 1395.
46. Tanniru, M.; Yuan, Q.; Misra, R. D. K. Polymer 2006, 47, 2133.
47. Yuan, Q.; Misra, R. D. K. Polymer, 2006, 47, 4421.
48. Yuan, Q.; Jiang, W.; An, L. J.; Misra, R. D. K. J Appl Polym Sci, to appear.
49. Lie, S.; Yu, Y.; Cui, Y.; Zhang, H. F.; Mo, Z. S. J Appl Polym Sci 1998, 70, 2371.